NASA Technical Memorandum 86037

Flow Field Survey Near the Rotational Plane of an Advanced Design Propeller on a JetStar Airplane

Kevin Robert Walsh

December 1985

National Aeronautics and
Space Administration

NASA Technical Memorandum 86037

Flow Field Survey Near the Rotational Plane of an Advanced Design Propeller on a JetStar Airplane

Kevin Robert Walsh
Ames Research Center, Dryden Flight Research Facility, Edwards, California

1985

National Aeronautics and
Space Administration
Ames Research Center
Dryden Flight Research Facility
Edwards, California 93523

SUMMARY

An investigation was conducted to obtain upper fuselage surface static pressures and boundary layer velocity profiles below the centerline of an advanced design propeller. This investigation documented the upper fuselage velocity flow field in support of the in-flight acoustic tests conducted on a JetStar airplane. Initial results of the boundary layer survey showed evidence of an unusual flow disturbance, which was attributed to the two windshield wiper assemblies on the aircraft. The assemblies were removed, eliminating the disturbance from the flow field.

This report presents boundary layer velocity profiles at altitudes of 6096 and 9144 m (20,000 and 30,000 ft) and Mach numbers from 0.6 to 0.8, and it investigates the effects of windshield wiper assemblies on these profiles. Because of the unconventional velocity profiles that were obtained with the assemblies mounted, classical boundary layer parameters, such as momentum and displacement thicknesses, are not presented. The effects of flight test variables (Mach number and angles of attack and sideslip) and an advanced design propeller on boundary layer profiles — with the wiper assemblies mounted and removed — are presented.

INTRODUCTION

Advanced design propellers, described in reference 1, are intended to provide substantial improvements in propeller cruise efficiency at low transonic speeds. One concern, however, is passenger acceptance of the noise levels generated by these propellers operating at supersonic tip speeds (refs. 2,3). Because accurate wind tunnel acoustic measurements are difficult to obtain (ref. 1), in-flight acoustic measurements were obtained for three different advanced design propellers (refs. 4 to 6). These flight tests were conducted at NASA Ames Research Center's Dryden Flight Research Facility using the JetStar airplane as a carrier vehicle. Flight-obtained acoustic data for the SR-2 and SR-3 advanced design propellers were compared with theoretical predictions (ref. 7). Flight data for the SR-2, SR-3, and SR-6 propellers were compared with wind tunnel test results (refs. 4 to 6).

In support of the acoustic flight test program and to validate the flow-field model used for the theoretical acoustic predictions (ref. 7), upper fuselage surface static pressures and boundary layer total pressures were measured below the propeller. Local flow conditions at the propeller centerline and free-stream locations were measured as described in reference 8.

During the flight test program, unusual boundary layer profiles were obtained. These profiles were attributed to flow disturbances generated by each of the two aircraft windshield wiper assemblies. The assemblies were removed, resulting in typical boundary layer profiles. These flow field data will be used to improve the acoustic predictions.

This report presents the JetStar aircraft upper fuselage boundary layer velocity profiles and investigates the effects of windshield wiper assemblies on the velocity profiles. The effects of flight test variables, such as Mach number and angles of attack and sideslip — with the windshield wiper assemblies mounted and removed — are presented. Velocity ratio contours, obtained from the boundary layer measurements,

are used to develop a conceptual flow model approximating the disturbance generated by the windshield wiper assemblies. Also shown is the effect of an advanced design propeller on the velocity profiles. Because of the unconventional velocity profiles that were obtained with the assemblies mounted, classical boundary layer parameters, such as momentum and displacement thicknesses, are not presented.

NOMENCLATURE

C_L	centerline
C_p	pressure coefficient
F.S.	fuselage station, cm (in)
H_p	pressure altitude, m (ft)
M	noseboom Mach number
M_{pcl}	Mach number at the centerline of the advanced design propeller
M_y	Mach number as a function of height above the fuselage
P_{sl}	local static pressure, kN/m^2 (psid)
$P_{s_{pcl}}$	static pressure at the propeller centerline, kN/m^2 (psid)
U_y/U_{pcl}	local boundary layer probe velocity/velocity at the centerline of the advanced design propeller
X/L	nondimensional distance from airplane nose
y	height above the fuselage, cm (in)
α	angle of attack, deg
β	angle of sideslip, deg

CARRIER AIRCRAFT AND PROPELLER

The JetStar airplane (fig. 1), used in the acoustic and flow-field tests, is a medium-range jet transport that can accommodate up to 10 passengers. It is powered by four JT12A-6 turbojet engines.

Figure 1(a) is a three-view drawing of the JetStar airplane showing the location of an advanced design propeller. The propeller was mounted on a pylon that was offset from the vertical centerline by 8°. Table 1 lists the locations of the aircraft components and instrumentation and their nondimensional distance from the aircraft nose. The propeller centerline is 80.8 cm (31.8 in) above the fuselage

surface. The propeller plane is 685.0 cm (269.7 in) from the nose of the aircraft and 441.2 cm (173.7 in) from the windshield wiper assemblies. The overall length of the JetStar airplane is 1841.5 cm (725.0 in). Figure 1(b) is a head-on photograph of the JetStar airplane showing the advanced design propeller and the windshield wiper assemblies. The geometry of the windshield wiper housings is 7.6 cm (3.0 in) high, 10.2 cm (4.0 in) long, and 3.8 cm (1.5 in) wide at its maximum width.

Three advanced propeller designs were flown during the acoustic test program. For this study, flow field data were obtained using the 10-bladed, SR-6 propeller. This propeller has a nominal diameter of 69.6 cm (27.4 in). It was designed for a cruise Mach number of 0.8 at a tip speed of 213 m/sec (700 ft/sec), which resulted in a helical tip Mach number of 1.07. The tip of the propeller was swept approximately 40° for aerodynamic and acoustic benefits. A photograph of the SR-6 propeller with the boundary layer rakes is shown in figure 2. Reference 3 discusses some design characteristics of the SR-6 propeller. Design characteristics of four other advanced designed propellers are given in reference 1.

INSTRUMENTATION

Seven surface static orifices, two boundary layer rakes, a pylon-mounted air data probe, and a noseboom air data probe were used to obtain the flow-field velocity profiles near the fuselage station of the SR-6 advanced design propeller.

For ease of reference, the locations of the aircraft components and instrumentation are shown in table 1.

Surface Static Pressure Orifices

Seven surface static pressure orifices were installed on the upper fuselage below the advanced design propeller. They were placed in existing microphone ports in the fuselage skin, as shown in figure 3. Two of the orifices were located just forward of each of the two boundary layer rakes.

Boundary Layer Rakes

The boundary layer rakes were mounted on the aircraft fuselage 10 cm (3.9 in) aft of the rotational plane of the propeller, as shown in figure 3. Both rakes were 695.0 cm (273.6 in) from the nose of the airplane and 451.2 cm (177.6 in) from the windshield wiper assemblies. The 12.7-cm (5.0-in) boundary layer rake was installed 15.4 cm (6.1 in) left of the fuselage centerline. The 20.3-cm (8.0-in) rake was installed 14.0 cm (5.5 in) to the right of the fuselage centerline.

Drawings of the two rakes are shown in figure 4. The 12.7-cm (5.0-in) boundary layer rake (fig.4(a)) had 12 total pressure probes, each having two outer probes with inlets angled 45° to the flow direction for determining flow angularity. Only data from the center probes were used for this report. The 20.3-cm (8.0-in) boundary layer rake (fig. 4(b)) had nine single total pressure probes, each with an inside chamfer of 30°. Photographs of the rake installations for the various configurations tested can be seen in figures 2 and 5.

Pylon Air Data Probe

A pitot static pressure probe, equipped with a flow direction vane system, was mounted on the pylon in place of the propeller air turbine drive motor (fig. 5). This probe, used for two test flights, obtained accurate static and total pressures to determine the reference conditions for the boundary layer measurements. The static pressure orifices were in the same vertical plane as the propeller plane of rotation. The centerline of the probe was aligned parallel to the centerline of the removed propeller air turbine drive motor, which was inclined down 3° from the fuselage reference line. Additional details about this probe and its installation are given in reference 8.

Aircraft Air Data Probe

A pitot static pressure probe, designed for flight research, and equipped with a flow direction vane system was mounted on the noseboom of the JetStar aircraft. Wind tunnel tests confirmed the minimal sensitivity of the static pressure orifices to changes in angles of attack up to 15° (ref. 9).

Instrumentation Hookup and Accuracies

Figure 6 is a diagram of the instrumentation hookup for the two rakes and the seven surface static pressure orifices. Two 32-port electronically scanned, multiple-pressure transducer assemblies measured 62 differential pressures. The transducer assemblies were referenced to a common source, which was measured by an absolute pressure transducer. The reference pressure was a fuselage static pressure that was approximately equal to ambient static pressure. A pressure tank was used to damp any pressure fluctuations in the reference system.

The differential transducers that were used had ranges of ± 17.24 kN/m^2 (± 2.5 psid) and 0 to 34.47 kN/m^2 (0 to 5.0 psid). All transducers were located in the JetStar cabin, which was temperature controlled. The transducer accuracies obtained were ± 0.2 percent of full scale or approximately ± 1.5 percent in terms of velocity ratio.

A description and the accuracies of the air data measurements are discussed in reference 8.

TEST PROCEDURE

Configurations

Flow distributions were obtained for three configurations:

1. With the windshield wiper assemblies mounted and the propeller removed.

2. With the windshield wiper assemblies removed and the propeller removed.

3. With the windshield wiper assemblies removed and the propeller mounted and operating.

The data obtained with the propeller operating were obtained from windmill-to-operating rpm. Only the operating rpm results are presented in this paper.

Flight Conditions

For all configurations tested, flow distributions were obtained at the following conditions:

1. An altitude of 6096 m (20,000 ft), Mach numbers of 0.6 and 0.7, and an angle-of-attack range of 2.9° to 3.6°.

2. An altitude of 9144 m (30,000 ft), Mach numbers of 0.6, 0.7, and 0.8, and an angle-of-attack range of 2.7° to 5.2°.

For these flight conditions, sideslip angles of approximately 0°, ±2°, and ±4° were obtained.

DATA REDUCTION AND ANALYSIS

Data were time averaged over 4-second intervals to minimize transient effects in the data. The intervals were chosen so Mach number and angles of attack and sideslip changes were minimal. All intervals analyzed had a sampling rate of 25 samples per second.

Indicated noseboom and propeller centerline Mach numbers were computed using the respective noseboom and pylon probe static and total pressures. Position-error corrections were applied to the noseboom as discussed in reference 8. For flights where the pylon probe was installed, a calibration curve between the free-stream Mach number and the propeller centerline Mach number was obtained. For flights without the pylon probe, the calibration curve determined the propeller centerline Mach number from the noseboom Mach number.

Boundary layer probe Mach numbers were derived from probe total pressures and the surface static pressures measured in front of each rake. Static port number 1 was used for the 20.3-cm (8.0-in) rake, and static port number 6 for the 12.7-cm (5.0-in) rake. It was assumed that the static pressure and total temperature within the boundary layer were constant. The probe Mach numbers were then converted into probe velocities. The velocity ratio was computed using the following equation:

$$\frac{U_y}{U_{pcl}} = \frac{M_y}{M_{pcl}} \left[\frac{1 + 0.2\,(M_{pcl})^2}{1 + 0.2\,(M_y)^2} \right]^{\frac{1}{2}}$$

The velocity at the propeller centerline was chosen as the reference velocity because when the windshield wipers were installed, all probes of the two boundary layer rakes were influenced by a disturbance. This disturbance prevented defining the edge, or reference, velocity of the rakes.

The velocity ratios obtained for all test configurations were plotted as a function of the height of the rake probes for the two rakes. A compilation of velocity ratio as a function of height data at Mach 0.8 and an altitude of 9144 m (30,000 ft) was obtained as a function of sideslip angle. These data were used to map velocity ratio contours at each rake as a function of sideslip. By combining the velocity ratio contours for both the 20.3-cm (8.0-in) and the 12.7-cm (5.0-in) rakes, a conceptual flow model at 0° sideslip was developed.

RESULTS AND DISCUSSION

The first results show pressure coefficients of the seven surface static orifices with the windshield wiper assemblies mounted and removed. The boundary layer velocity ratio profiles obtained with the assemblies removed are shown; the effects of angle of attack and Mach number on those profiles are discussed. The velocity ratio profiles obtained with the assemblies mounted are then compared with the profiles obtained with the assemblies removed; the effects of Mach number and angles of attack and sideslip, are discussed. A conceptual flow model, at the given flight condition with the wiper assemblies mounted, is developed, based on sideslip data, to assist in the interpretation of results with the assemblies mounted.

The primary emphasis on the data presented corresponds to the design conditions (Mach 0.8 and an altitude of 9144 m (30,000 ft)) of an advanced design propeller. Data shown at other conditions represent the best comparisons available.

Surface Static Pressures

Pressure coefficients of the seven surface static orifices, at the given flight condition and with the windshield wiper assemblies mounted and removed, are shown in figure 7. The pressure coefficients with the assemblies removed (solid symbols) were lower than with the assemblies mounted (open symbols). Static port 4, located right of the fuselage centerline (X/L = 0.372), had a significantly higher pressure coefficient than all other static ports for both the assemblies mounted and removed. This deviation was attributed to the static port not being flush to the fuselage skin; it was not used to determine the local static pressure.

Boundary Layer Velocity Ratio Profiles

Windshield wiper assemblies removed – Boundary layer velocity ratio profiles measured at the 20.3-cm (8.0-in) and the 12.7-cm (5.0-in) rakes (with the assemblies removed) are presented in figure 8 at the given flight conditions. The boundary layer height is approximately 12 cm (4.7 in) for the 20.3-cm (8.0-in) rake. The difference between the two curves is considered insignificant.

Effect of angle of attack: Figure 9 shows the effect of angle of attack on the boundary layer velocity profile for the 20.3-cm (8.0-in) rake at Mach 0.72. No significant effect is shown for the angle-of-attack range tested.

Effect of Mach number: Figure 10 presents boundary layer profiles at Mach 0.62, 0.75, and 0.80 while maintaining an angle of attack of 3.5°. As Mach number increased, the velocity ratio decreased.

Comparison with windshield wiper assemblies mounted and removed — Figure 11 compares the velocity ratio profiles at Mach 0.8 with the windshield wiper assemblies mounted and removed. The assemblies had a significant effect on the boundary layer velocity profiles. Both the 20.3-cm (8.0-in) rake, (fig. 11(a)) and the 12.7-cm (5.0-in) rake, (fig. 11(b)) show similar trends. This disturbance is believed to be caused by a vortex generated from each of the two windshield wiper assemblies. These vortices energized the boundary layer by increasing its velocity approximately 10 percent in the 1- to 4-cm (0.5- to 1.5-in) region while decreasing the velocity up to 15 percent at a height of 12 cm (4.7 in). The disturbance extends above the upper limit of the 20.3-cm (8.0-in) rake.

Similar data from the 20.3-cm (8.0-in) rake for a range of Mach numbers at two altitudes are shown in figure 12. There are some small differences, but, in general, the effect of the windshield wiper assemblies on the flow field is significant.

Effect of angle of attack: Figure 13 shows the effects of angle of attack on the velocity ratio profiles for the 20.3-cm (8.0-in) rake with the assemblies mounted. At Mach 0.62, an increase in angle of attack from 3.6° to 4.8° has some effect on the boundary layer velocity profile, unlike data in figure 9 obtained with the wiper assembies removed. At the higher angle of attack, the vortex flow appears to be lifted farther above the fuselage surface.

Effect of Mach number: The effect of Mach number on the velocity ratio profiles for the 20.3-cm (8.0-in) rake with the assemblies mounted is shown in figure 14. An increase from Mach 0.72 to 0.81, at an angle of attack of 2.6°, decreases the velocity ratio profile, similar to the data of figure 10 obtained with the wiper assemblies removed.

Effect of sideslip: Comparison of data obtained with the wiper assemblies mounted and removed show that sideslip angles not only have a large impact on velocity ratio profiles, but also create differences between the boundary layer rakes (fig. 15). At 2° of sideslip (fig. 15(a)), with the assemblies mounted, the 12.7-cm (5.0-in) rake shows a large decrease in velocity ratio, while the 20.3-cm (8.0-in) rake shows no effect. At -2° of sideslip the opposite results occur: the 20.3-cm (8.0-in) rake shows a large decrease in velocity ratio, while the 12.7-cm (5.0-in) rake shows no effect.

Figure 16 is an illustration of how the vortices appear to respond to changes in sideslip. At 0° of sideslip, a vortex is generated from each windshield wiper assembly and propagates downstream, impacting each rake. At 2° of sideslip, the vortex generated from the right assembly propagates to the 12.7-cm (5.0-in) rake, which is on the left side of the fuselage centerline, while the vortex generated from the left assembly misses both rakes. The 20.3-cm (8.0-in) rake does not encounter the vortex flow at 2° of sideslip. Although not shown in figure 16, the opposite effect occurs at -2° of sideslip.

At greater angles of sideslip, the vortices would be expected to miss both rakes. Data in figure 17 at ±4° of sideslip supports this and shows little difference between data obtained with the assemblies mounted or removed.

Velocity ratio contours with assemblies mounted: Using the velocity ratios for the ranges of sideslip angles tested, a contour plot, obtained from the 20.3-cm (8.0-in) rake, was developed to visualize the flow disturbance (fig. 18). For reference, the fuselage skin is at a height of 0 cm (0 in) and the 20.3-cm (8.0-in) rake is located at the zero-degree-of-sideslip condition. For different sideslip angles at the given flight condition, the value of the velocity ratios were recorded on the figure as a function of its height. Constant lines of velocity ratio were then drawn. The solid symbols along the abscissa in figure 18 represent the angles of sideslip where data were obtained.

Note the two lobes of velocity ratios in figure 18. They are symmetric about a -1.25° sideslip angle. The lobes are centered at approximately the 0° and the -2.25° sideslip conditions, which correspond to the velocity ratio profiles shown in figures 11(a) and 15(b), respectively. The disturbance diminishes at sideslip angles greater than 1.75°. This is consistent with figure 15(a), where at $\beta = 2°$, no effect is shown for the 20.3-cm (8.0-in) rake with the wiper assemblies mounted. Recalling that the 20.3-cm (8.0-in) rake is located to the right of the fuselage centerline, the lobe centered about the -2.25° of sideslip is the result of the vortex generated from the left windshield wiper assembly.

Figure 19 presents a similar constant velocity ratio contour obtained from the 12.7-cm (5.0-in) rake. The dashed contour lines are an estimation, based on the experience gained by drawing the lines of constant velocity ratios for the 20.3-cm (8.0-in) rake. Again, the solid symbols along the abscissa represent the angles of sideslip where data were obtained.

The two lobes of velocity ratios in the contour plot are approximately symmetric about the 1.25° sideslip angle. The areas of reduced velocity ratios are approximately centered about the 0.5° and the 2° sideslip angles. This corresponds to the large effects on the velocity ratio profiles shown in figures 11(b) and 15(a) for the 12.7-cm (5.0-in) rake.

Conceptual flow model: Figure 20, a conceptual flow model of the vortices, presents data that are a combination of the constant velocity ratio contours of the 20.3-cm (8.0-in) rake from -1.25° to 4° of sideslip (fig. 18) and the contours of the 12.7-cm (5.0-in) rake from -4° to 1.25° of sideslip (fig. 19). The perceived general rotation of this complex vortex flow is shown by the arrows.

Depending on the fuselage location, the 0.95-velocity ratio line may be as close as 4 cm (1.6 in) or as far as 20 cm (7.8 in) above the fuselage surface. Reference 10 discusses the significant impact that the disturbance had on the acoustic measurements.

A similar analysis was conducted to map the effects of sideslip with the wiper assemblies removed. Figure 21 shows a profile that is free of any disturbances.

Effect of Advanced Design Propeller

Figure 22 compares boundary layer velocity profiles obtained with the SR-6 advanced design propeller operating at cruise power and with the propeller removed. Data at several conditions showed that the propeller had no effect on the boundary

layer velocity profiles. Similar effects would be expected with the SR-2 and SR-3 advanced design propellers because their diameters are smaller than the SR-6 propeller, increasing the distance between the propeller tip and the upper fuselage boundary layer.

CONCLUSIONS

Flow distributions near the rotational plane of an advanced design propeller on a JetStar airplane were measured. The significant conclusions are:

1. With the windshield wiper assemblies mounted, unusual boundary layer profiles were obtained. These profiles were attributed to a disturbance believed to be a vortex generated from each windshield wiper assembly.

These vortices energized the boundary layer by increasing its velocity approximately 10 percent in the 1- to 4-cm (0.5- to 1.5-in) region while decreasng the velocity up to 15 percent at a height of 12 cm (4.7 in). The disturbance extended above the upper limit of the 20.3-cm (8.0-in) rake.

2. With the windshield wiper assemblies removed, a conventional boundary layer profile existed. The boundary layer height was approximately 12 cm (4.7 in).

3. The SR-6 advanced design propeller had no effect on the boundary layer velocity profiles.

Ames Research Center
Dryden Flight Research Facility
National Aeronautics and Space Administration
Edwards, California 93523, February 13, 1984

REFERENCES

1. Jeracki, Robert J.; Mikkelson, Daniel C.; and Blaha, Bernard J.: Wind Tunnel Performance of Four Energy Efficient Propellers Designed for Mach 0.8 Cruise. NASA TM-79124, 1979.

2. Dittmar, James H.; Jeracki, Robert J.; and Blaha, Bernard J.: Tone Noise of Three Supersonic Helical Tip Speed Propellers in A Wind Tunnel. NASA TM-79167, 1979.

3. Dittmar, James H.; Stefko, George L.; and Jeracki, Robert J.; Noise of the 10-Bladed, 40° Swept SR-6 Propeller in A Wind Tunnel. NASA TM-82950, 1982.

4. Dittmar, James H.; and Lasagna, Paul L.: A Preliminary Comparison Between the SR-3 Propeller Noise in Flight and in A Wind Tunnel. NASA TM-82805, 1982.

5. Dittmar, James H.; Lasagna, Paul L.; and Mackall, Karen G.: A Preliminary Comparison Between the SR-6 Propeller Noise in Flight and in a Wind Tunnel. NASA TM-83341, 1983.

6. Lasagna, Paul L.; Mackall, Karen G., and Cohn, Robert B.: In-Flight Acoustic Test Results for the SR-2 and SR-3 Advanced-Design Propellers. AIAA Paper 83-1214, June 1983.

7. Farassat, F.; Martin, R. M.; and Greene, G. C.: Noise Prediction for JetStar Prop-Fan Test. NASA TM-81916, 1980.

8. Webb, Lannie D.: Mach Number and Flow Field Calibration at the Advanced Design Propeller Location on the JetStar Airplane. NASA TM-84923, 1985.

9. Richardson, Norman R.; and Pearson, Albin O.: Wind Tunnel Calibrations of a Combined Pitot-Static Tube, Vane Type Flow Direction Transmitter, and Stagnation-Temperature Element at Mach Numbers From 0.60 to 2.87. NASA TND-122, 1959.

10. Brooks, B.M.; and Mackall, K.G.: Measurement and Analysis of Acoustic Flight Test Data for Two Advanced Design High-Speed Propeller Models. AIAA Paper 84-0250, Jan. 1984.

TABLE 1. — LOCATIONS OF AIRCRAFT COMPONENTS AND INSTRUMENTATION

Description	Fuselage station, cm (in)	Nondimensional distance from aircraft nose, X/L
Aircraft nose	238.8 (94.0)	0
Windshield wiper assemblies	482.6 (190.0)	0.132
Surface static orifices		
Row 1	907.8 (357.4)	0.363
Row 2	923.8 (363.7)	0.372
Propeller rotation plane	923.8 (363.7)	0.372
Boundary layer rakes	933.8 (367.6)	0.377

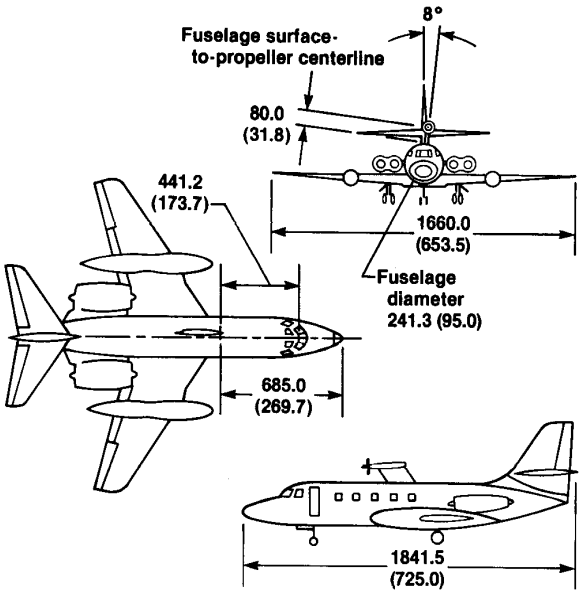

(a) Three-view drawing of the JetStar airplane. Dimensions are in centimeters (inches).

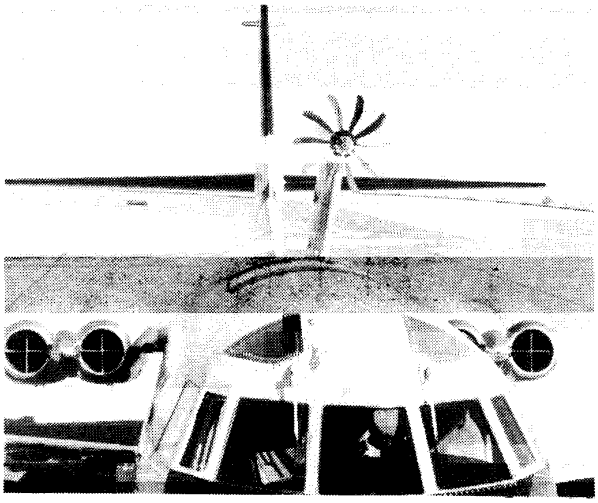

ECN 18052

(b) The JetStar airplane.

Figure 1. JetStar test airplane with the SR-6 advanced design propeller installed.

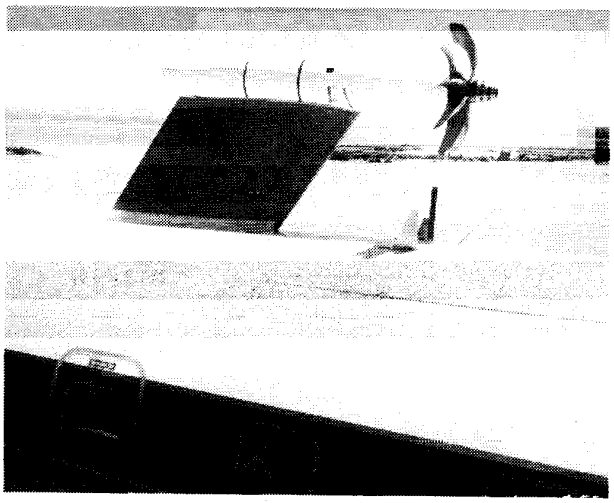

ECN 18510

Figure 2. The SR-6 advanced design propeller and boundary layer rakes.

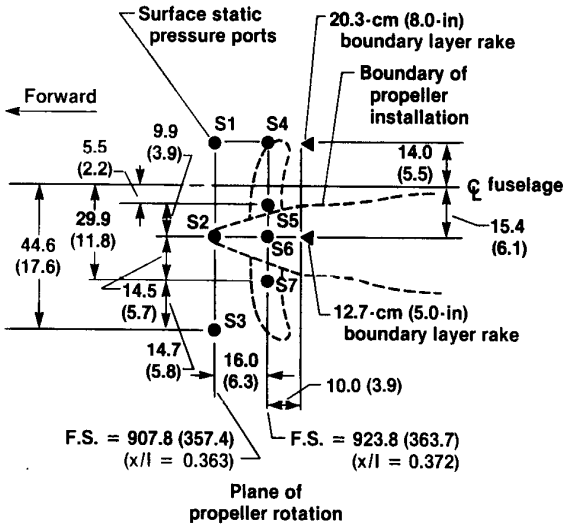

Figure 3. Top view of the surface static ports and the boundary layer rakes. Dimensions are in centimeters (inches).

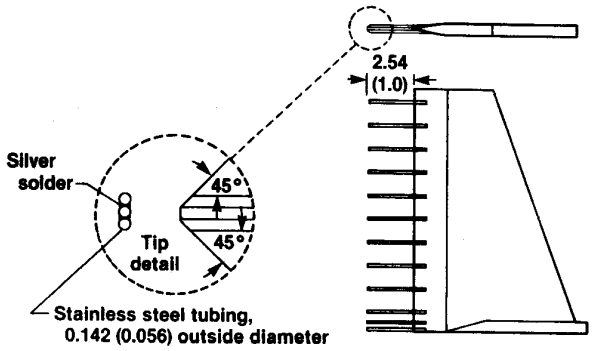

(a) 12.7-cm (5.0-in) rake.

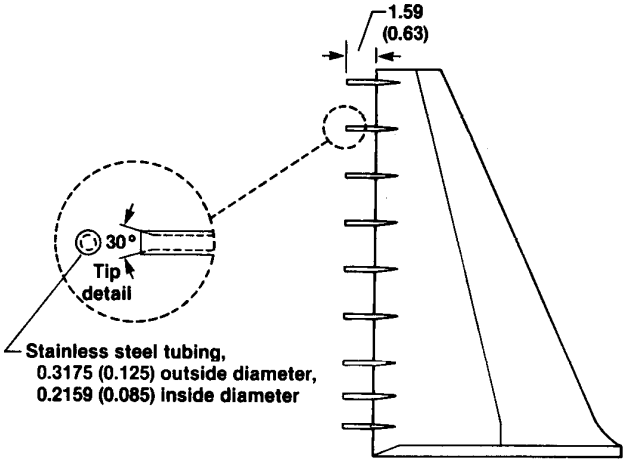

(b) 20.3-cm (8.0-in) rake.

Figure 4. Schematic of boundary layer rakes showing some design criteria. Dimensions are in centimeters (inches).

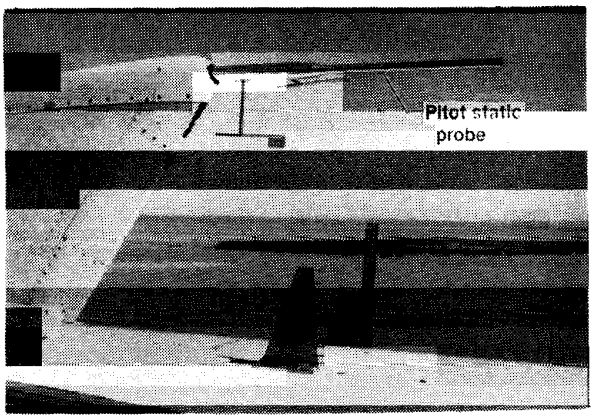

Figure 5. Photograph of pylon-mounted pitot static probe.

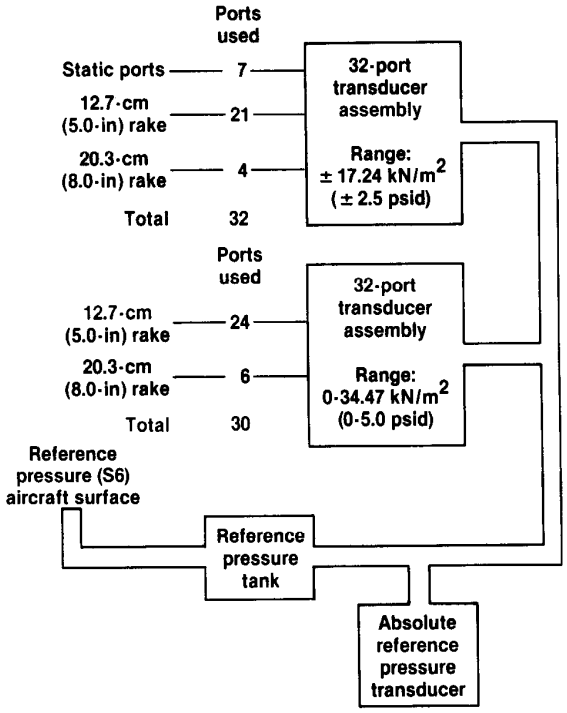

Figure 6. Diagram of the pressure measurement system.

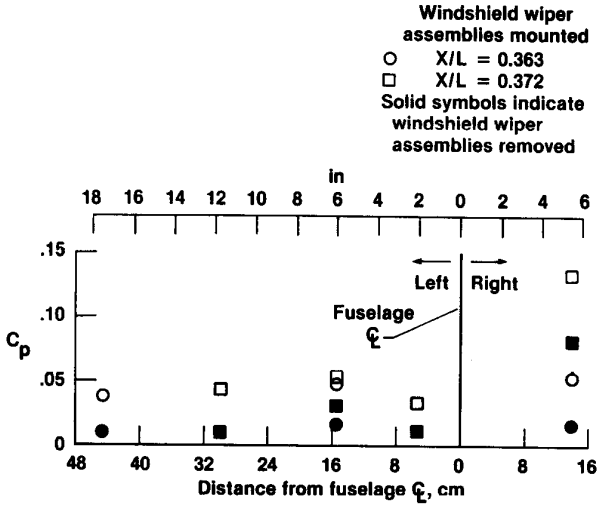

Figure 7. Pressure coefficients for the seven surface static orifices with windshield wiper assemblies mounted and removed. M = 0.8, H_p = 9144 m (30,000 ft).

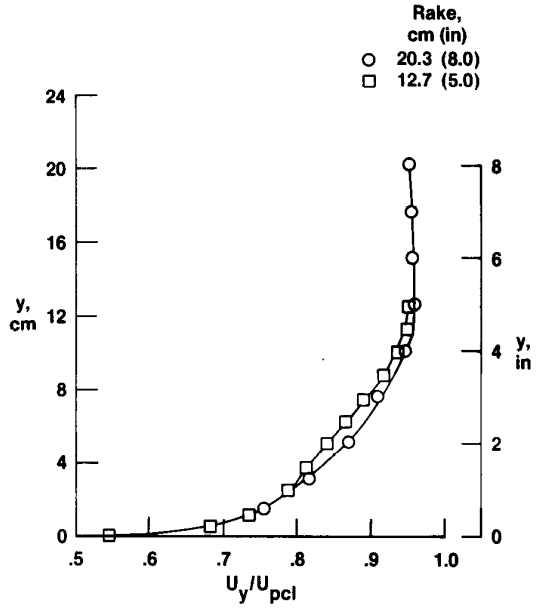

Figure 8. Boundary layer velocity ratio profile with the windshield wiper assemblies removed. H_p = 9144 m (30,000 ft); M = 0.8; α = 2.7°; β ≈ 0°.

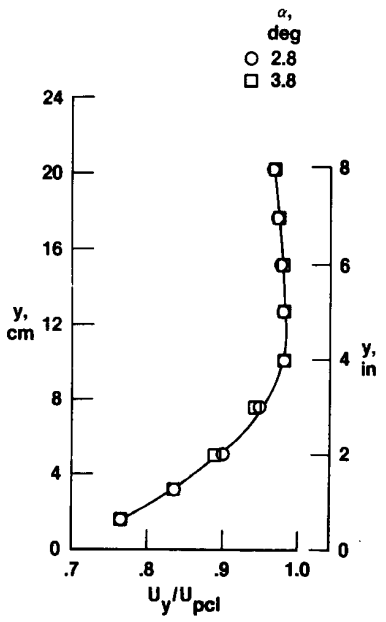

Figure 9. Boundary layer velocity ratio profiles for the 20.3-cm (8.0-in) rake showing the effect of angle of attack with the windshield wiper assemblies removed. H_p = 6096 m (20,000 ft); m = 0.72; β ≈ 0°.

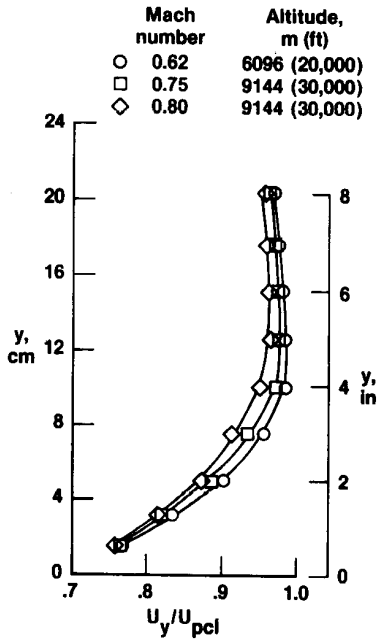

Figure 10. Boundary layer velocity ratio profiles for the 20.3-cm (8.0-in) rake showing the effect of Mach number with windshield wiper assemblies removed. α ≈ 3.5°; β ≈ 0°.

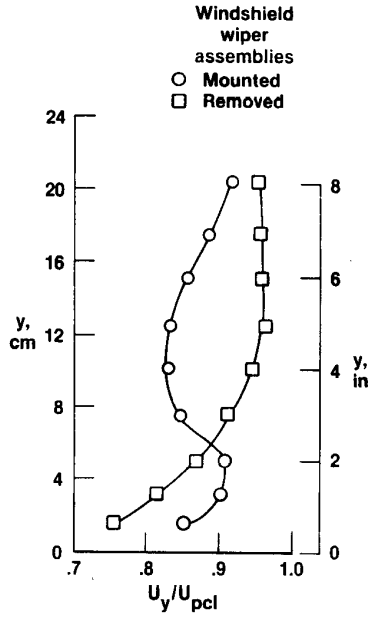

(a) 20.3-cm (8.0-in) rake.

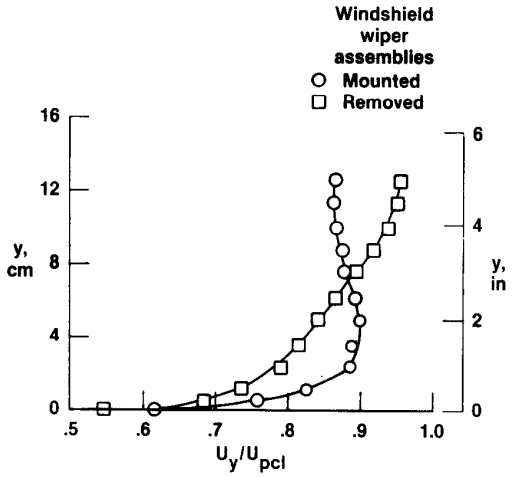

(b) 12.7-cm (5.0-in) rake.

Figure 11. Boundary layer velocity ratio profiles showing the effect of the windshield wiper assemblies mounted and removed. $M = 0.8$; $\beta \approx 0°$; $\alpha = 2.7°$; $H_p = 9144$ m (30,000 ft).

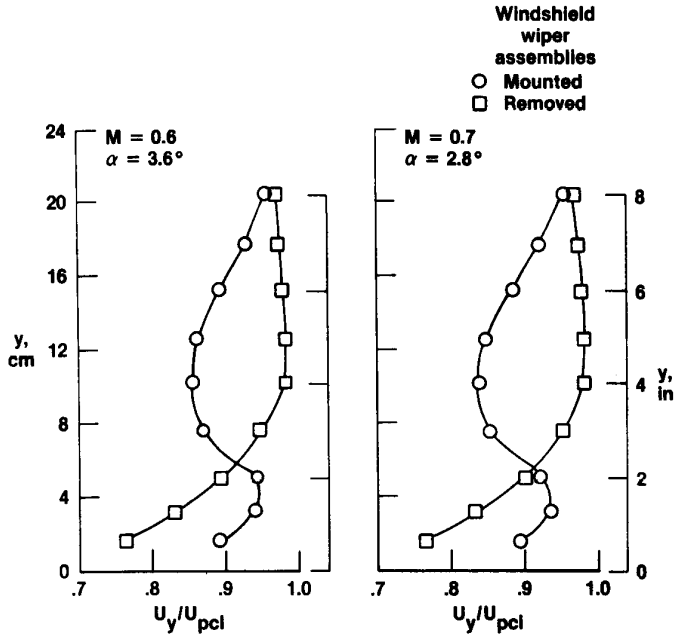

(a) H_p = 6096 m (20,000 ft).

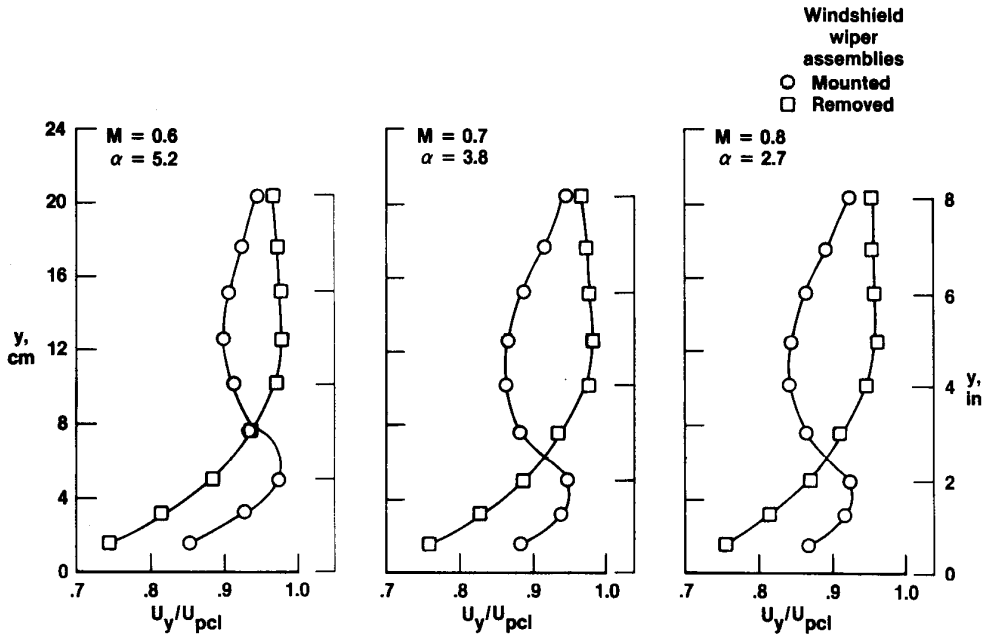

(b) H_p = 9144 m (30,000 ft).

Figure 12. Boundary layer velocity ratio profiles for the 20.3-cm (8.0-in) rake showing the effect of the windshield wiper assemblies mounted and removed at different flight conditions. β ≈ 0°.

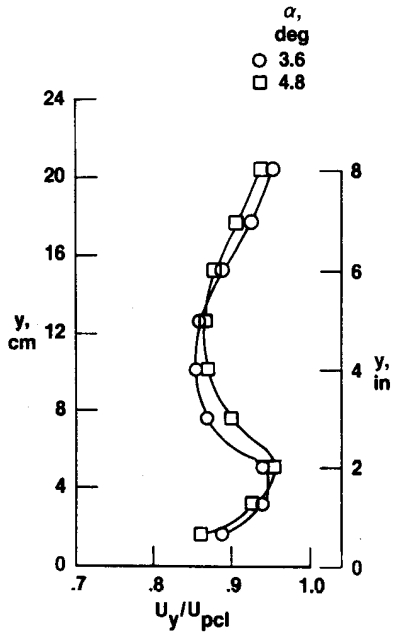

Figure 13. Boundary layer velocity ratio profiles showing the effect of angle of attack with windshield wiper assemblies mounted. H_p = 6096 m (20,000 ft); M = 0.62; β ≈ 0°.

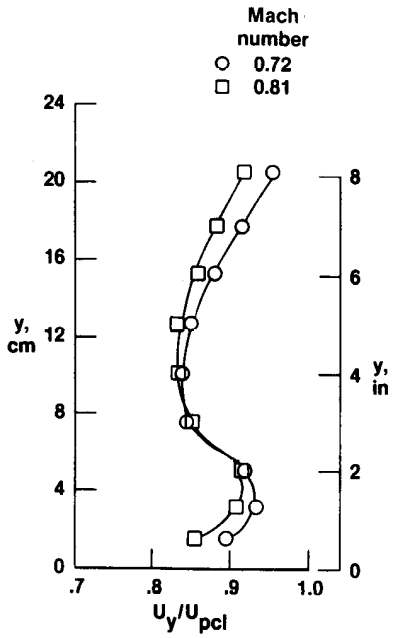

Figure 14. Boundary layer velocity ratio profiles showing the effect of Mach number with windshield wiper assemblies mounted. H_p = 6096 m (20,000 ft); α = 2.6°; β ≈ 0°.

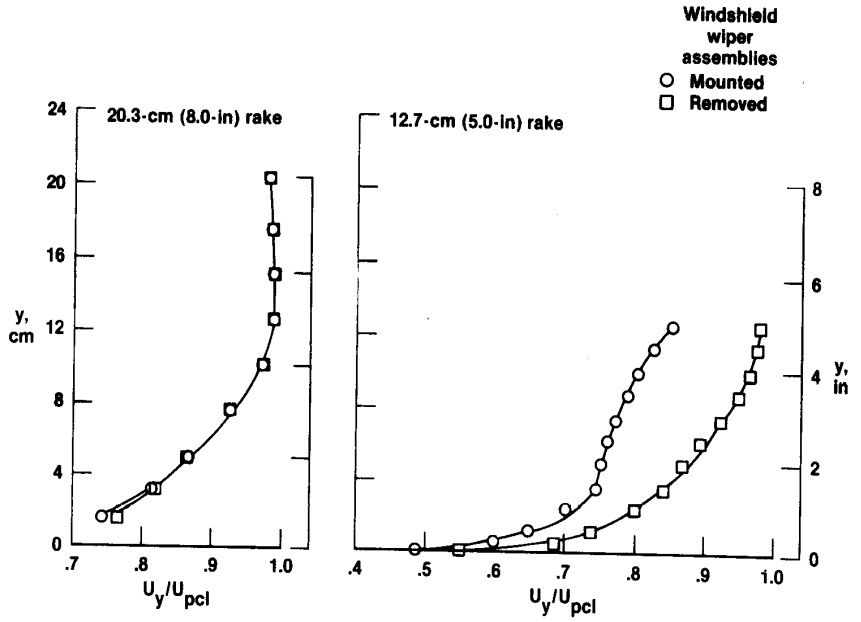

(a) $\beta = 2°$.

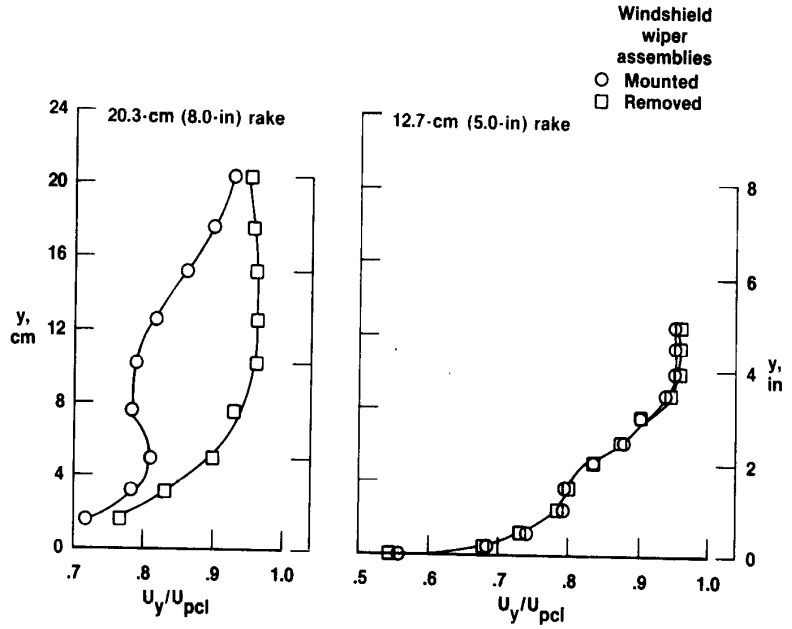

(b) $\beta = -2°$.

Figure 15. Boundary layer velocity ratio profiles for both boundary layer rakes showing the effect of angle of sideslip with the windshield wiper assemblies mounted and removed. H_p = 9144 m (30,000 ft); M = 0.8; $\alpha = 3.0°$.

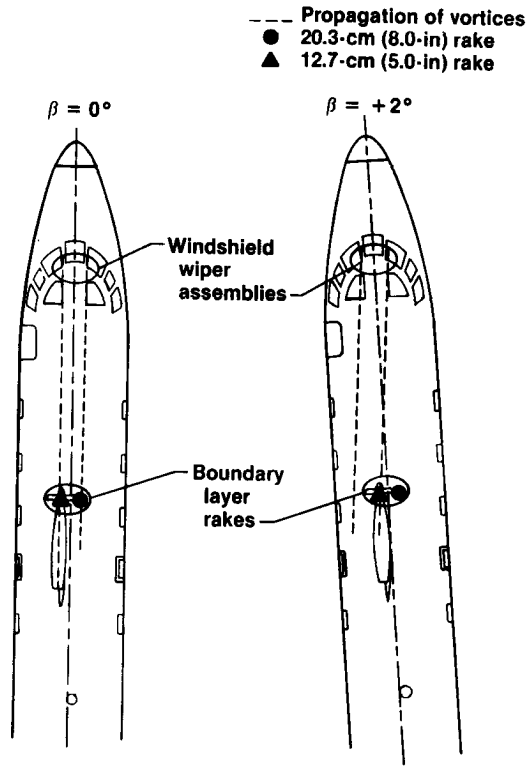

Figure 16. Illustration of the vortices propagating at two sideslip angles.

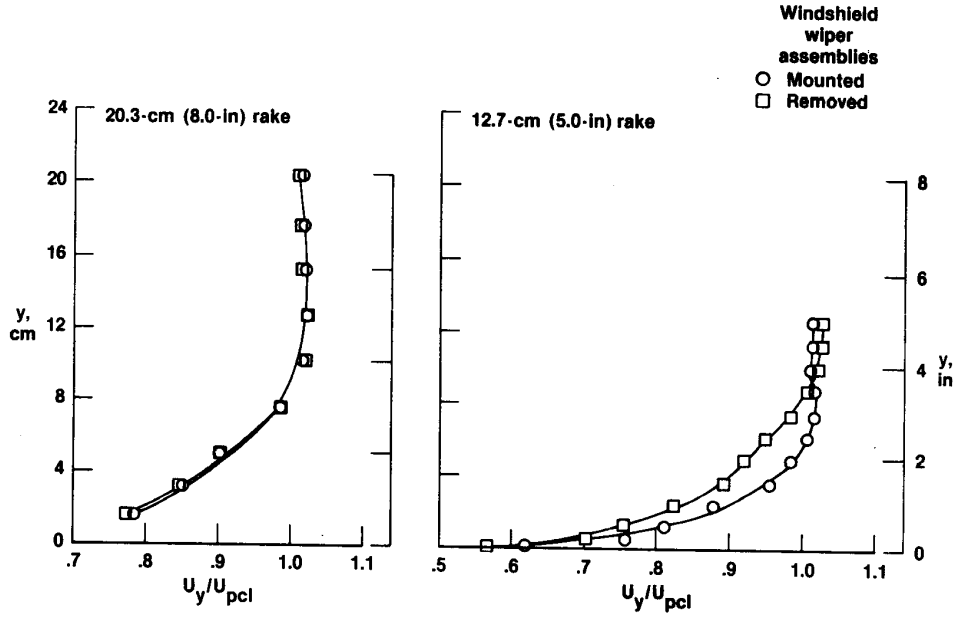

(a) $\beta = 4°$.

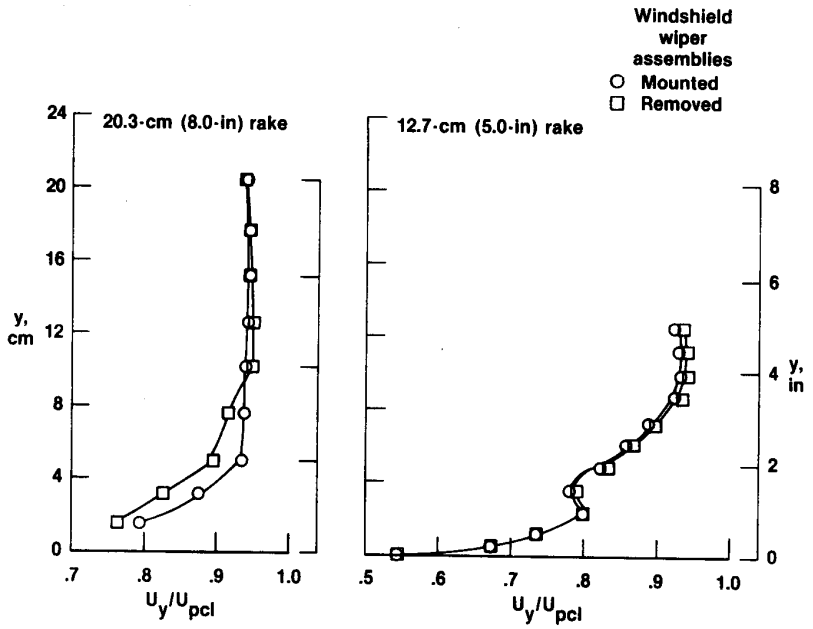

(b) $\beta = -4°$.

Figure 17. Boundary layer velocity ratio profiles for both boundary layer rakes showing the effects of angle of sideslip with the windshield wiper assemblies mounted and removed. H_p *= 9144 m (30,000 ft);* $M = 0.8$; $\alpha = 3.0°$.

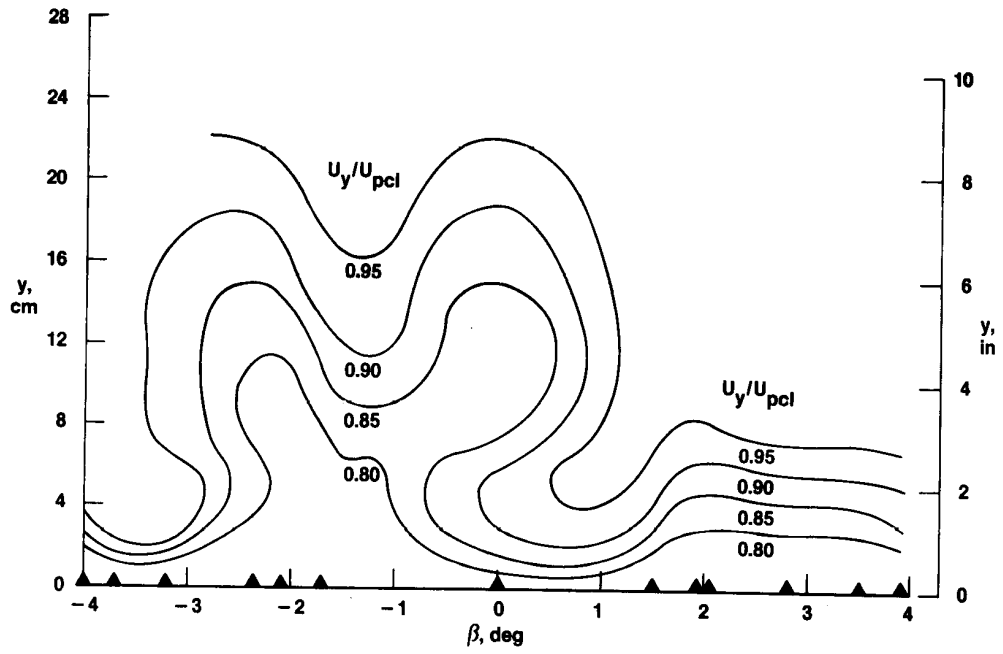

Figure 18. Velocity ratio contours from the 20.3-cm (8.0-in) rake at various sideslip angles with windshield wiper assemblies mounted. H_p = 9144 m (30,000 ft), M ≈ 0.8; α, from 2.7° to 3.4°.

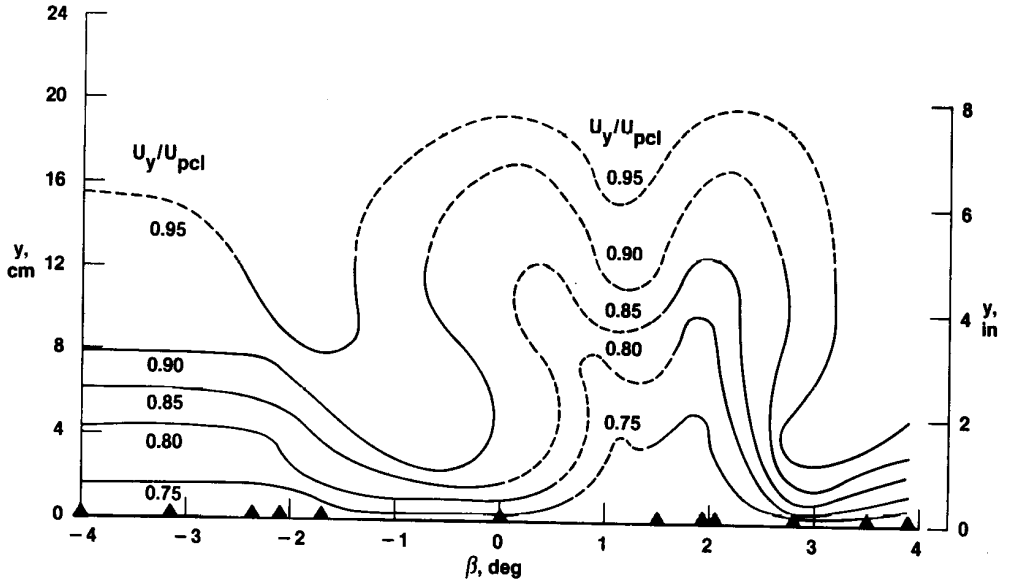

Figure 19. Velocity ratio contours from the 12.7-cm (5.0-cm) rake at various sideslip angles with windshield wiper assemblies mounted. H_p = 9144 m (30,000 ft), M ≈ 0.8, α, from 2.7° to 3.4°.

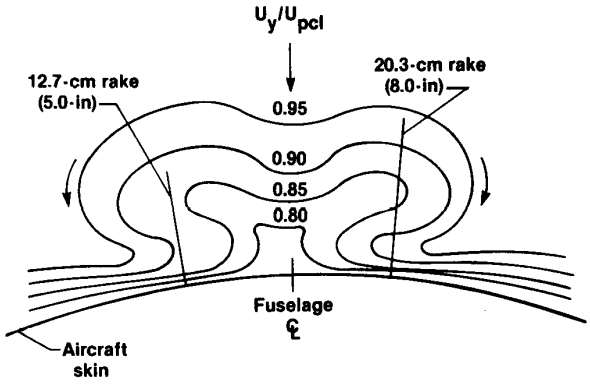

Figure 20. Conceptual flow model with windshield wiper assemblies mounted. H_p = 9144 m (30,000 ft); M ≈ 0.8, α, from 2.7° to 3.4°.

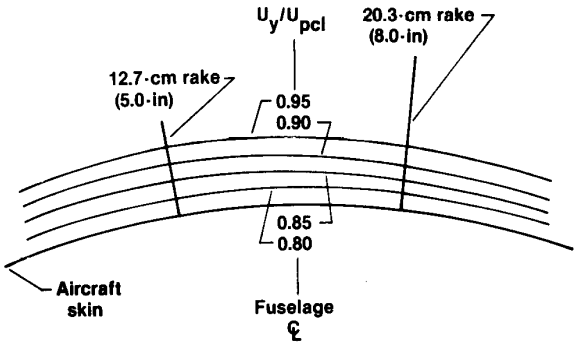

Figure 21. Conceptual flow model with windshield wiper assemblies removed. H_p = 9144 m (30,000 ft), M ≈ 0.8, α, from 2.8° to 3.2°.

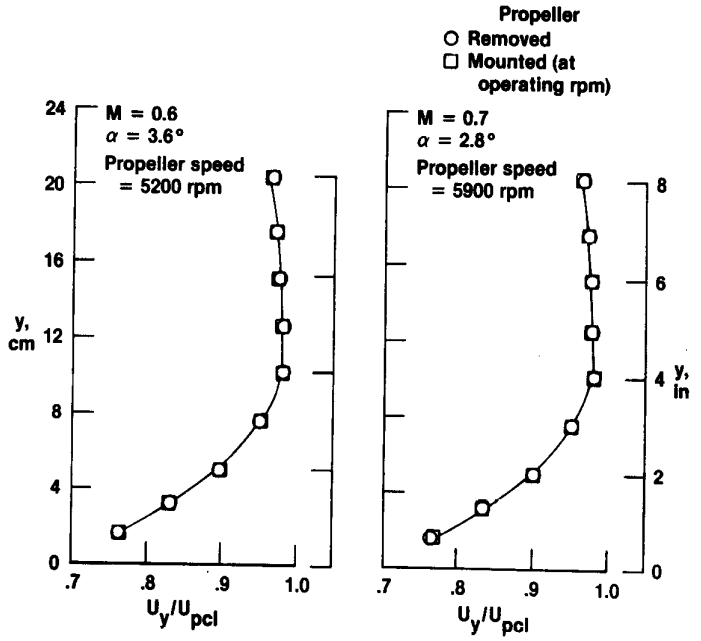

(a) H_p = 6096 m (20,000 ft).

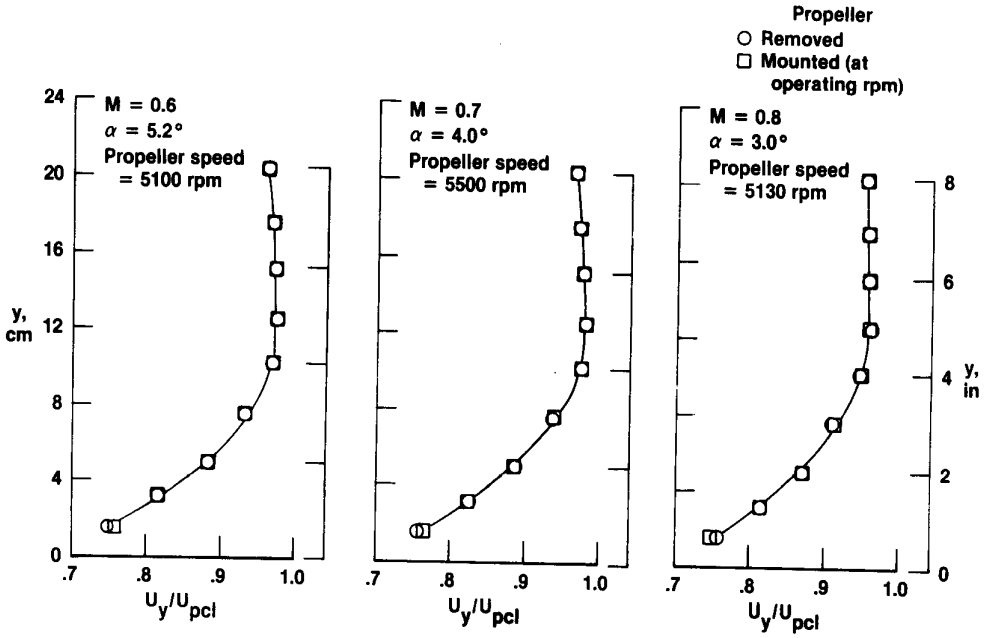

(b) H_p = 9144 m (30,000 ft).

Figure 22. Boundary layer velocity ratio profiles showing the effects of the advanced design propeller mounted and removed. $\beta \approx 0°$.

1. Report No.	2. Government Accession No.	3. Recipient's Catalog No.
NASA TM-86037		

4. Title and Subtitle	5. Report Date
FLOW FIELD SURVEY NEAR THE ROTATIONAL PLANE OF AN ADVANCED DESIGN PROPELLER ON A JETSTAR AIRPLANE	December 1985
	6. Performing Organization Code
7. Author(s) Kevin Robert Walsh	8. Performing Organization Report No. H-1226
	10. Work Unit No. RTOP 535-03-11
9. Performing Organization Name and Address NASA Ames Research Center Dryden Flight Research Facility P.O. Box 273 Edwards, California 93523	11. Contract or Grant No.
	13. Type of Report and Period Covered Technical Memorandum
12. Sponsoring Agency Name and Address National Aeronautics and Space Administration Washington D.C. 20546	14. Sponsoring Agency Code

15. Supplementary Notes

16. Abstract

An investigation was conducted to obtain upper fuselage surface static pressures and boundary layer velocity profiles below the centerline of an advanced design propeller. This investigation documented the upper fuselage velocity flow field in support of the in-flight acoustic tests conducted on a JetStar airplane. Initial results of the boundary layer survey showed evidence of an unusual flow disturbance, which was attributed to the two windshield wiper assemblies on the aircraft. The assemblies were removed, eliminating the disturbances from the flow field.

This report presents boundary layer velocity profiles at altitudes of 6096 and 9144 m (20,000 and 30,000 ft) and Mach numbers from 0.6 to 0.8, and it investigates the effects of windshield wiper assemblies on these profiles. Because of the unconventional velocity profiles that were obtained with the assemblies mounted, classical boundary layer parameters, such as momentum and displacement thicknesses, are not presented. The effects of flight test variables (Mach number and angles of attack and sideslip) and an advanced design propeller on boundary layer profiles — with the wiper assemblies mounted and removed — are presented.

17. Key Words (Suggested by Author(s))	18. Distribution Statement
Advanced design propeller Fuselage aerodynamics Boundary layers Velocity profiles	Unclassified-Unlimited STAR category 02

19. Security Classif. (of this report)	20. Security Classif. (of this page)	21. No. of Pages	22. Price*
Unclassified	Unclassified	26	A03

For sale by the National Technical Information Service, Springfield, Virginia 22161